

# The characterization of mixed titanate $Ba_{1-x}Sr_xTiO_3$ phase formation from oxalate coprecipitated precursor

S. Suasmoro<sup>a,\*</sup>, S. Pratapa<sup>a</sup>, D. Hartanto<sup>b</sup>, D. Setyoko<sup>b</sup>, U.M. Dani<sup>c</sup>

<sup>a</sup>Department of Physics, Faculty of Mathematics and Natural Sciences, Surabaya Institute of Technology “10 November”, Surabaya 60111, Indonesia

<sup>b</sup>Department of Chemistry, Faculty of Mathematics and Natural Sciences, Surabaya Institute of Technology “10 November”, Surabaya 60111, Indonesia

<sup>c</sup>Material Science Research Center, National Atomic Energy Agency, Kawasan Puspitek Serpong, Tangerang 15314, Indonesia

Received 10 February 1999; received in revised form 14 April 1999; accepted 11 May 1999

## Abstract

Mixed titanates  $Ba_{1-x}Sr_xTiO_3$  were synthesized via calcination of oxalate coprecipitated precursors. On heating there were three thermal event occurred:  $T < 250^\circ C$  corresponds to the evaporation of trapped water and dehydration,  $T = 250^\circ C - 450^\circ C$  corresponds to the decomposition of oxalate and the formation of an intermediate phase where the composition is close to  $[Ba_{1-x}Sr_x]_2Ti_2O_5.CO_3$  and  $T = 600^\circ C - 700^\circ C$  corresponds to the carbonate decomposition and the formation of  $Ba_{1-x}Sr_xTiO_3$  phase. Powders calcined at  $T = 700^\circ C$  for 2 h are single phase, have grain size ranges of 0.2–2  $\mu m$  and elongated morphology. Rietveld refinements of the XRD data showed single phase of perovskite structure in which their tetragonality decreased with increasing concentration of  $Sr^{2+}$  incorporated in  $Ba^{2+}$  site. The transition temperature showed strong correlation with the tetragonality. © 2000 Elsevier Science Ltd. All rights reserved.

**Keywords:**  $BaTiO_3$ ; Calcination; Perovskites; Powders-chemical preparation; X-ray methods

## 1. Introduction

Mixed titanate  $Ba_{1-x}Sr_xTiO_3$  is a ferroelectric material which has a perovskite structure and posses high dielectric constant and high resistivity. These characteristics promise applications of the material such as for capacitor, positive temperature coefficient (PTC), infra red sensor, electrooptic device, and recently for DRAM (dynamic random access memory). By reason of these widely applications of the material, an effort on its synthesis and material forming is still attractive.<sup>1–5</sup>

There are two principles for the preparation: (a) dry synthesis by solid state reaction of oxide and carbonates, (b) wet chemical synthesis such as coprecipitation, sol-gel, polymerization. In dry synthesis, a solid state reaction between  $TiO_2$  and  $MCO_3$  (M bivalent metal) releases  $CO_2$  which can intervene in the kinetics of the reaction. This technique of preparation has advantages, e.g. easy preparation and realization of desired cation proportion in the compound. On the contrary, the reaction occurs at high temperature,  $T = 1000^\circ C - 1300^\circ C$ ,

which cause agglomeration and grain growth. To achieve the desired characteristics such as high dielectric constant, mechanical strength, and fine microstructure, it is necessary to start with preparing fine and narrow size distribution powder. For this reason, agglomeration and grain growth must be highly reduced, it can be achieved by calcination at relatively low temperature, fine and homogeneous precursors.<sup>6</sup> One of the methods for preparing precursors for this purpose is the wet chemical route such as oxalate coprecipitation.

The principles of the coprecipitation technique comprise a reaction of highly soluble salts such as  $MCl_2$  and  $M'Cl_4$  and oxalic acid  $H_2C_2O_4$  yields a precipitate. For  $M = Ba$  and  $M' = Ti$ , the procedure has been established,<sup>7</sup> however, the description of phase change on heating is still in discussion. Reed<sup>8</sup> showed that the precursors became  $BaCO_3$  and  $TiO_2$  before titanate formation, while Bernier<sup>9</sup> found an intermediate phase  $BaTiO_3 \cdot \frac{1}{2} CO_3$  before titanate formation. Leitte et al.<sup>10</sup> explained that for a precursor prepared, based on the Pechini method for  $x = 1$ , the intermediate phase of  $Sr_2Ti_2O_5.CO_3$  was formed before titanate phase formation. Kumar et al.,<sup>11</sup> on the other hand found similar results, the intermediate phase for  $x = 0$  was  $Ba_2Ti_2O_5.CO_3$ . It is important to identify the phenomena

\* Corresponding author. Tel./fax: +62-31-594-3351.

E-mail address: suasm@its.ac.id (S. Suasmoro).

(e.g. thermal events, phase changes) associated with the formation of the mixed titanate. The objectives of this work are then to characterize the phase change of the mixed precursors after heat treatment, the formation of mixed titanate  $\text{Ba}_{1-x}\text{Sr}_x\text{TiO}_3$ , and characterization of calcined powder.

## 2. Experimental

Raw materials,  $\text{TiCl}_4$ ,  $\text{BaCl}_2 \cdot 2\text{H}_2\text{O}$ ,  $\text{SrCl}_2 \cdot 2\text{H}_2\text{O}$  and  $\text{H}_2\text{C}_2\text{O}_4 \cdot 2\text{H}_2\text{O}$  were reagent grade supplied by E. Merck. The schedule of the experiment was a variation in  $x$  to make a composition  $\text{Ba}_{1-x}\text{Sr}_x\text{TiO}_3$ . The precursors,  $(\text{Ba}/\text{Sr})\text{TiO}(\text{C}_2\text{O}_4)_2 \cdot 4\text{H}_2\text{O}$ , were prepared by mixing  $\text{TiOCl}_2$  obtained by water addition on  $\text{TiCl}_4$  and  $\text{Ba}/\text{SrCl}_2$  solution in one batch with  $\text{H}_2\text{C}_2\text{O}_4$  saturated solution at the temperature kept at  $T = 40^\circ\text{C} - 45^\circ\text{C}$ . The precipitate material was then separated by filtration followed by demineralized water washing to eliminate  $\text{Cl}^-$ . To evaluate the completeness of washing,  $\text{AgNO}_3$  tests have been performed, followed by drying at  $T = 110^\circ\text{C}$ .

Experimental studies of mixed titanate formation have been conducted by simultaneous Simadzu DT30 differential thermal analyses (DTA) and thermogravimetric analysis (TGA) with heating rate  $10^\circ\text{C}/\text{min}$ , JEOL JDX3530 X-ray diffraction (XRD) and JASCO5300 Fourier transform infra red (FT-IR) of heat treated samples (heating rate  $5^\circ/\text{min}$ ). Rietveld refinements using LHPM software<sup>12</sup> were carried out to evaluate the lattice parameters. In this case, the input parameters for refinements were tetragonal perovskite structure,  $a = b = 4.0025\text{Å}$  and  $c = 4.0232\text{Å}$ , P4mm space group and the atomic coordinates [Ba,Sr] (000); Ti ( $\frac{1}{2}, \frac{1}{2}, 0.512$ ); O ( $0, \frac{1}{2}, \frac{1}{2}, 0, 0.0026$ ). To examine the morphology and size of the calcined powder the PHILIPS-525M scanning electron microscope (SEM) was utilized. Finally, to determine the Curie temperature, an ANDO AG-4311 LCR meter was used. To monitor the variation of capacitance, samples were put in a temperature-controlled heated reservoir. The measurement conditions were 500 Hz, 1.5 V and heating rate  $1^\circ\text{C}/\text{min}$ .

## 3. Results and discussion

The present method of synthesis is promising to obtain a high quality powder due to good mixing and reaction. It is believed that the precursor contains a mixture of  $(1-x)\text{BaTiO}(\text{C}_2\text{O}_4)_2 \cdot 4\text{H}_2\text{O}$  and  $x\text{SrTiO}(\text{C}_2\text{O}_4)_2 \cdot 4\text{H}_2\text{O}$ . Examination of samples by inductive coupled plasma spectroscopy (ICPS) indicates that the values of  $x$  varies about 1% from initially planned in which the tendencies of  $(\text{Ba} + \text{Sr})/\text{Ti}$  atomic content ratio are slightly higher than 1. Once the precursors are obtained, the following are then powders which are

readily subjected to the thermal analyzer. Fig. 1 shows DTA and TGA for different  $x$ . There are three thermal events observed: below  $250^\circ\text{C}$ , between 250 and  $450^\circ\text{C}$ , and between 600 and  $700^\circ\text{C}$ .

### 3.1. The first thermal event ( $T < 250^\circ\text{C}$ )

This is endothermic accompanied by weight loss of 14–17%, which is clearly due to the evaporation of trapped water in the cavity and the dehydration process. At this temperature the result was  $\text{Ba}/\text{SrTiO}(\text{C}_2\text{O}_4)_2$ . XRD examination of samples heat treated at  $T = 250^\circ\text{C}$  shows that the powders are amorphous, Fig. 2(A).

### 3.2. The second thermal event ( $T = 250 - 450^\circ\text{C}$ )

TGA results show a simple weight loss. If the sample mass at  $T = 250^\circ\text{C}$  is taken as a new reference, this weight loss is about 31% for  $x = 0$  and 35% for  $x = 0.3$ . The corresponding DTA result shows alternating endothermic–exothermic phenomena.

The endothermic phenomenon is caused by the breaking-off of oxalate bonding and released CO gas. Afterward, the gas reacts instantaneously with oxygen in air causing an exothermic phenomenon<sup>13</sup>. These two instantaneous events superposed result in an alternating endothermic–exothermic occurrence. The role of Sr has been studied by precursors containing high concentration Sr and indicated that the endothermic part decreased with increasing  $x$  and vanished for  $x = 1$ . This demonstrate that the oxalate in  $[\text{SrTiO}]^{4+}$  is more weakly bounded than in  $[\text{BaTiO}]^{4+}$ .

Considering that the reaction underlying the thermal events is controlled by the thermal decomposition at the surface and obeys linear kinetics then it proceeds following Kingery et al.,<sup>14</sup> the enthalpy of the decomposition should be estimated. The results were  $\Delta H = 25\text{ kJ/}$

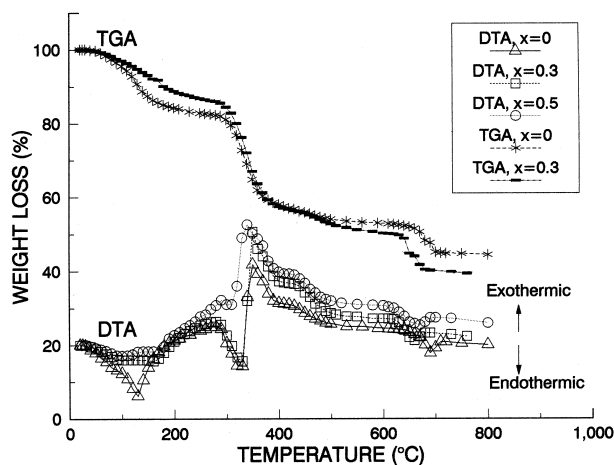


Fig. 1. Thermal analysis of precursors  $\text{Ba}_{1-x}\text{Sr}_x\text{TiO}(\text{C}_2\text{O}_4)_2 \cdot 4\text{H}_2\text{O}$  with heating rate  $10^\circ\text{C}/\text{min}$ .

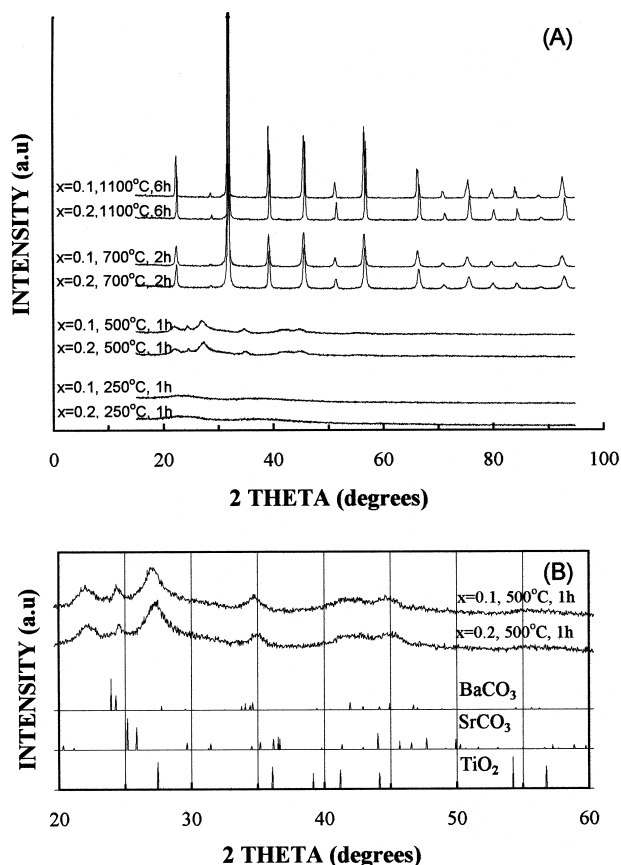


Fig. 2. (A) XRD patterns of phase change after heat treatment. (B) Search match for samples heat treated at  $T=500^\circ\text{C}$  for 1 h.

mol for  $x=0$  and  $\Delta H=30\text{kJ/mol}$  for  $x=0.3$ . These values can be compared to that of decomposition of  $\text{BaCO}_3/\text{SrCO}_3$  which are typically  $80\text{ kJ/mol}$  and occur at high temperature. The low enthalpies of the decomposition indicate the low formation probability of barium or strontium carbonates at this temperature range.<sup>10</sup>

XRD analysis of samples after heat treatment at  $T=500^\circ\text{C}$  soaked for 1 h has been performed to examine the phase change after gas release, Fig. 2(A). Peaks are clearly observed indicating that both samples are crystallized. Examination of phase by comparison with JCPDS data showed that the probable composition as indicated by Reed,<sup>8</sup>  $\text{BaCO}_3$ ,  $\text{SrCO}_3$ ,  $\text{TiO}_2$  were not found, Fig. 2(B). Therefore, these individual carbonates and oxide of titanium were not formed after thermal phenomenon. This explanation support the thermal analysis conclusion as discussed above.

Further analysis by FT-IR of the treated samples ( $T=500^\circ\text{C}$ , 1 h), Fig. 3, shows absorption peaks of the vibration characteristics of  $\text{CO}_3^{2-}$  carbonate group.<sup>10</sup> There is no remarkable role of  $x$  on absorption peaks even though for high  $x$ , Table 1. This indicates that the bonding energies are similar for all cases. The vibration characteristic lower than  $800\text{ cm}^{-1}$  is known as a characteristic of metal–oxygen bonding in the compound.

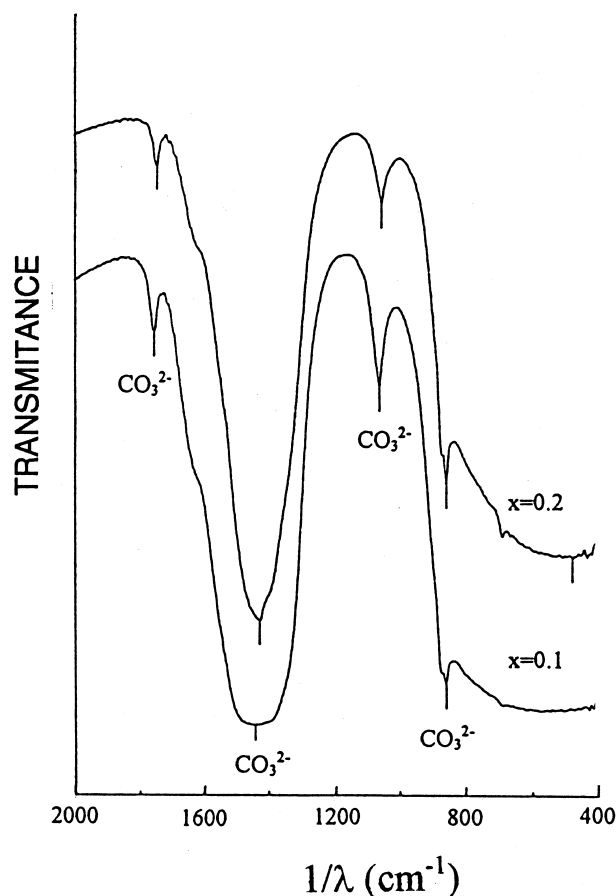


Fig. 3. FT-IR absorption pattern of the precursors heated at  $T=500^\circ\text{C}$  for 1 h.

Table 1  
Absorption peaks of FT-IR ( $1/\lambda - \text{cm}^{-1}$ ) for precursors heated at  $500^\circ\text{C}$  for 1 h

$x=0$	$x=0.1$	$x=0.2$	$x=0.5$	$x=1$	$x=1^a$
858	858	858	858	858	850
1059	1061	1063	1061	1061	1073
1424	1426	1443	1440	1440	1450
1751	1752	1755	1760	1760	1770

<sup>a</sup> Data from Ref. 10.

These data indicate that the material contain carbonate bonding, however, it is small probability resulted from Ba or Sr carbonate as is discussed in thermal and XRD analysis in the previous paragraphs. It was then supposed that an intermediary phase containing carbonate bonding exists in the samples.

Considering the TGA data, the intermediate phase should be  $(\text{Ba}_{1-x}\text{Sr}_x)_2\text{Ti}_2\text{O}_5\cdot\text{CO}_3$  with theoretical weight loss of 32% for  $x=0$  and 34% for  $x=0.3$  which are close to the experimental values, i.e. 31 and 35%. The result of the reaction supports Leitte et al.<sup>10</sup> for  $x=1$  and Kumar et al.<sup>11</sup> for  $x=0$ , however disagrees with Bernier<sup>9</sup> who explained that for  $x=0$  the results were  $\text{BaTiO}_3\cdot\frac{1}{2}\text{CO}_3$  and  $\text{CO}_2$

### 3.3. The third thermal event ( $T = 600\text{--}700^\circ\text{C}$ )

This is endothermic followed by weight loss of 9% for  $x=0$  and 11% for  $x=0.3$ . Considering that the calculated weight losses caused by decarbonation and released  $\text{CO}_2$  gas, were 9% for  $\text{BaTiO}_3$  and 10% for

Table 2  
Lattice parameter of  $\text{Ba}_{1-x}\text{Sr}_x\text{TiO}_3$  calcined at  $T = 700^\circ\text{C}$

Calcination (h)	$x$	Lattice parameter (Å)	
		$a$	$c$
2	0.2	3.98262	3.99721
4	0.2	3.98246	3.99685
2	0.1	3.99579	4.01194
4	0.1	3.99597	4.00956

$\text{Ba}_{0.7}\text{Sr}_{0.3}\text{TiO}_3$ . These values are in satisfactory agreement with the experimental data.

At  $T > 700^\circ\text{C}$  there is no more weight loss monitored by TGA. XRD analysis of calcined samples at  $T = 700^\circ\text{C}$  for 2 h with intermediate soaking 1 h at  $T = 500^\circ\text{C}$  confirmed that the samples are single phase, Fig. 2(A). However, a small peak was observed as an unidentified phase located at  $2\theta$  around  $28.57\text{--}28.77^\circ$ . The peak was not eliminated even though calcination was carried out at high temperature. It is speculated that this trace element is  $\text{Ba}_2\text{TiO}_4$  due to the fact that the samples have a slight excess of (Ba + Sr) as indicated by ICPS analysis. Apart from the impurity phase, the pattern shows a perovskite cubic structure designating that all  $\text{Sr}^{2+}$  are incorporated in  $\text{Ba}^{2+}$  sites. After a longer calcination dwell time (4 h), there was almost no

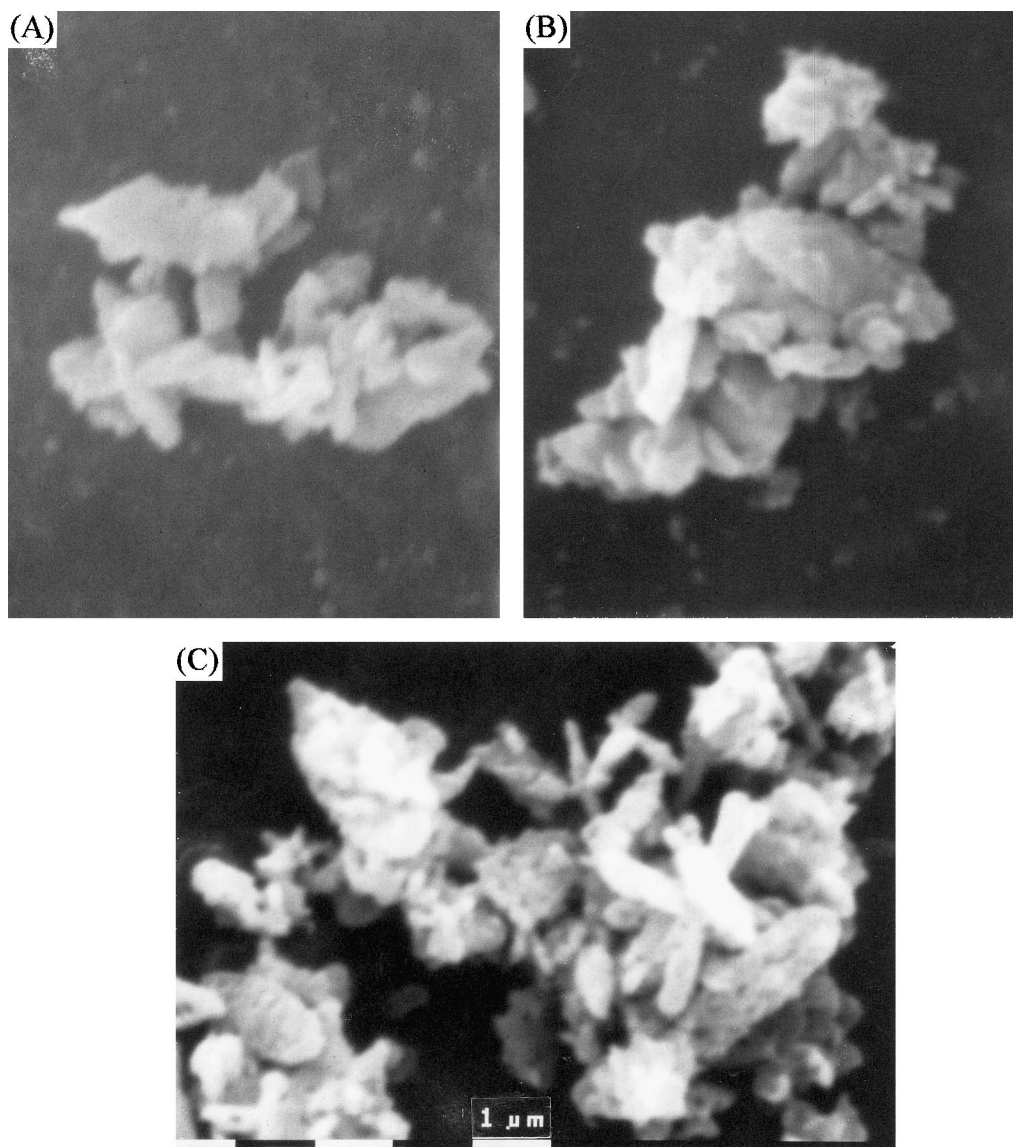


Fig. 4. SEM micrographs of  $\text{Ba}_{1-x}\text{Sr}_x\text{TiO}_3$  as calcined samples. (A) Calcination at  $T = 700^\circ\text{C}$ , 2 h for  $x=0$ ; (B) calcination at  $T = 700^\circ\text{C}$ , 2 h for  $x=0.2$ ; (C) calcination at  $T = 1100^\circ\text{C}$ , 6 h for  $x=0$ .

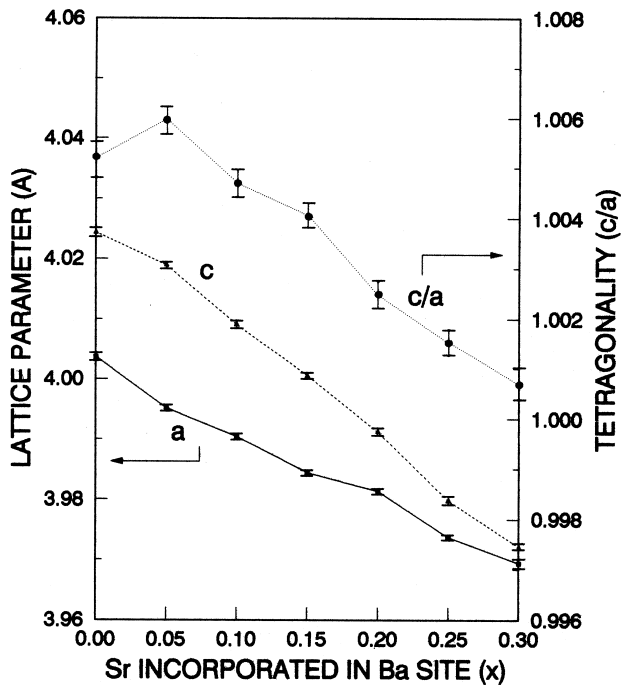


Fig. 5. Lattice parameters and tetragonality of samples calcined at  $T=1100^{\circ}\text{C}$  for 6 h.

difference in the resulting pattern. For further analysis, Rietveld refinements have been carried out. The acceptance of the refinement is based on the 'Figure of Merit' (FoM),  $R$  factors and goodness of fit GoF. In all cases, after final refinement, it was shown that  $R$ -Bragg  $< 6\%$ ,  $R$ -profile  $< 8\%$ ,  $R$ -weighted profile  $< 10\%$ ,  $R$ -expected profile  $< 7\%$  and GoF  $< 3\%$ . These values indicate that the refinements were successful and should be accepted. The results showed that the structure was tetragonal perovskite and their lattice parameter decreased with increasing dwell time, Table 2. A smaller lattice parameter for longer calcination should be due to better ionic rearrangement in the structure after decomposition. Furthermore, higher  $\text{Sr}^{2+}$  concentration incorporated in  $\text{Ba}^{2+}$  sites have reduced their lattice parameters.

Observations by SEM revealed that samples calcined at  $T=700^{\circ}\text{C}$  for 2 h have grain size ranges of 0.2–2  $\mu\text{m}$  in agglomerate form typically 5  $\mu\text{m}$  large with an elongated morphology, Fig. 4(A) and (B). It can be noted that there is no significant effect of  $\text{Sr}^{2+}$  substitution in the  $\text{Ba}^{2+}$  site vis a vis the morphology and size of powder. High calcination temperature  $T=1100^{\circ}\text{C}$  and longer soaking time  $t=6$  h induced grain growth, Fig. 4(C). The grains grew preferentially along the elongation axis.

Grain growth implies larger grain size, and has affected the shape of XRD peaks. Reflection peaks become sharper, hence doublets are distinguishable. Another mark from this data is the shifting of peaks to higher  $2\theta$  to become more significant when  $x$  increased, Fig. 2(A). This occurrence was probably due to the role of the Sr in the structure.

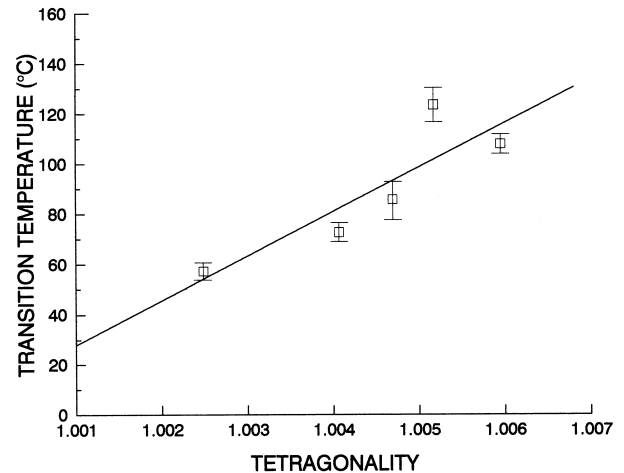


Fig. 6. Transition temperature against tetragonality for  $\text{Ba}_{1-x}\text{Sr}_x\text{TiO}_3$ .

The role of Sr incorporated in the structure should be studied on samples calcined at  $T=1100^{\circ}\text{C}$  with 6 h dwell time. Rietveld refinements of the XRD data revealed that lattice parameters vary with  $x$ , Fig. 5. Taking  $c/a$  as a degree of tetragonality of the structure, the data show that the tetragonality decreases and approaches unity with increasing  $x$ . The presence of  $\text{Sr}^{2+}$  in the  $\text{Ba}^{2+}$  site induced a new equilibrium denoting a shrinkage of both axis parameters in which the  $c$ -axis shrink more than the  $a$ -axis. It can be explained that the shrinkage of the axis should be due to the smaller ionic radius of  $\text{Sr}^{2+}$  (1.16 nm) than that of  $\text{Ba}^{2+}$  (1.36 nm). This signifies that the more the  $\text{Sr}^{2+}$  incorporated in  $\text{Ba}^{2+}$  sites, the more cubic the structure. It is consistent with the data that in the extreme case  $x=0$ ,  $\text{BaTiO}_3$  is tetragonal and for  $x=1$ ,  $\text{SrTiO}_3$  is cubic.

The degree of the tetragonality will have an effect on the temperature at which the cubic distortion occurred (transition temperature). The higher tetragonality requires higher energy to allow transition from tetragonal to cubic. Taking that the Curie temperature  $\theta_c$  as the transition temperature, the  $\theta_c$  measured from sintered pellets at  $T=1250^{\circ}\text{C}$  for 2 h has a strong linear correlation with the degree of tetragonality, Fig. 6. This dependency strengthened the conclusion that the  $\text{Sr}^{2+}$  ions have been well incorporated at the  $\text{Ba}^{2+}$  sites.

#### 4. Conclusion

The formation of mixed titanate from the oxalate coprecipitated precursors has been characterized. During heating, evaporation of trapped water and dehydration occurred below  $T=250^{\circ}\text{C}$ . Passing through the temperature range of  $T=250$ – $450^{\circ}\text{C}$  decomposition of oxalate occurred by releasing gases  $\text{CO}_2$  and  $\text{CO}$ , which instantaneously reacted with oxygen in air and resulted in alternating endothermic–exothermic phenomena.

During this stage an intermediate phase  $(\text{Ba}_{1-x}\text{Sr}_x)_2\text{Ti}_2\text{O}_5\cdot\text{CO}_3$  formed. The breaking-off of this carbonate started at  $T=600^\circ\text{C}$  and terminated at  $T=700^\circ\text{C}$  producing  $\text{CO}_2$  and the final product  $\text{Ba}_{1-x}\text{Sr}_x\text{TiO}_3$ .

Calcination at  $T=700^\circ\text{C}$  for 2 h revealed that the powders were single phase indicating that all  $\text{Sr}^{2+}$  incorporated in  $\text{Ba}^{2+}$  sites. These powders have a grain size of 0.2–2  $\mu\text{m}$  with elongated shape. Longer calcination at higher temperature has two effects, grain growth and slight reduction of lattice parameter. The more  $\text{Sr}^{2+}$  concentration incorporated in  $\text{Ba}^{2+}$  sites shrank the lattice parameter where the  $c$ -axis shrank more than the  $a$ -axis thus resulting with the tetragonality decreasing and approached to unity. This designates that the structure becomes more cubic, and lowers the transition temperature.

### Acknowledgements

The authors wish to acknowledge the Indonesian Ministry of Research and Technology for the financial support of this work. Thanks are also addressed to the Third World Academy of Science for the support on the initialization of work.

### References

1. Liu, W. T., Lakshmi Kumar, S. T., Knor, D. B., Lu, T. M. and Leeden, G. A., Deposition of amorphous  $\text{BaTiO}_3$  optical film at low temperature. *Appl. Phys. Lett.*, 1993, **63**(5), 574–576.
2. Komarov, A. V., Parkin, I. P. and Odlya, M., Self-propagating high-temperature synthesis of  $\text{SrTiO}_3$  and  $\text{Sr}_x\text{Ba}_y\text{TiO}_3$  ( $x+y=1$ ). *J. Mat. Sci.*, 1996, **31**, 5033–5037.
3. Parker, L. H. and Tasch, Al. F., Ferroelectric materials for 64Mb and 256 Mb DRAMs. *IEEE Circuits and Devices Mag.* Jan. 1990, 17–26.
4. Jida, S. and Miki, T., Electron paramagnetic resonance of Nb-doped  $\text{BaTiO}_3$  ceramics with positive temperature coefficient of resistivity. *J. Appl. Phys.*, 1996, **8**(9), 5234–5239.
5. Heywang, H. and Thomann, H., Positive temperature coefficient resistors. In *Electronic Ceramics*, ed. B. C. H. Steell. Elsevier Applied Science, London, 1991, pp. 29–48.
6. Suasmoro, S., Smith, D. S. and Lejeune, M., Influence of the mixing and calcination conditions on the characteristics of  $\text{YBa}_2\text{Cu}_3\text{O}_{(7-\delta)}$  powder. *Ceram. Int.*, 1992, **18**, 91–97.
7. Bernier, J. C., Poix, P. J. L. and Rhespringer, J. L., Procédé de préparation de gels thixotropes d'oxalates mixtes, et plus particulièrement d'un gel thixotrope d'oxalate double de titane et de baryum. French Patent. No. 2 570 373, 18 September 1986.
8. Reed, J. S., *Introduction to the Principles of Ceramics Processing*. John Wiley and Sons, New York, 1988, pp. 48–49.
9. Bernier, J. C., Chemical processing for electronic ceramic: a challenge. In *Ceramics Material Research*, ed. R. J. Brook. E-MRS, Amsterdam, 1989, pp. 233–241.
10. Leitte, E. R., Sousa, C. M. G., Longo, E. and Varela, J. A., Influence of polymerization on synthesis of  $\text{SrTiO}_3$ : Part I. Characteristics of polymeric precursors and their thermal decomposition. *Ceram. Int.*, 1995, **21**, 143–153.
11. Kumar, S., Messing, G. L. and White, W. B., Metal organic resin derived barium titanate: I. Formation of barium titanium oxycarbonate intermediate. *J. Am. Ceram. Soc.*, 1993, **76**(3), 617–624.
12. Hill, R. J. and Howard, C. J., *LHPM, Rietveld Refinement Program Manual*. Australian Atomic Energy Commission, Lucas Heights Research Laboratory, Menai, NSW, Australia, 1986.
13. Zhong, Z. and Gallagher, P. K., Combustion synthesis and characterization of  $\text{BaTiO}_3$ . *J. Mat. Sci.*, 1995, **10**(4), 945–952.
14. Kingery, W. D., Bowen, H. K. and Uhlmann, D. R. *Introduction to Ceramics*. 2nd edn. John Wiley and Sons, New York, 1976, pp. 443–444.